Quantitative Gait Assessment With Feature-Rich Diversity Using Two IMU Sensors

Yonatan Hutabarat, Dai Owaki, *Member, IEEE*, and Mitsuhiro Hayashibe, *Senior Member, IEEE*

***Abstract*—The importance of gait analysis in medical applications, such as in rehabilitation, has been widely studied. Wearable sensors have gained popularity owing to their convenience of use in a flexible environment, while providing accuracy and reliability, in comparison with the gold standard system, i.e., motion capture. In this study, we proposed a framework for quantitative gait assessment using only two inertial measurement unit (IMU) sensors, while extracting maximum number of features. Decreasing the number of sensors negatively affects the performance of gait assessment. However, through comparison with a motion capture setup and previous studies, we verified the potential and limitations of our proposed framework toward providing a compact sensing system with feature-rich diversity for gait assessment. The results revealed that the temporal differences were 4.22±15.48 ms (mean ± S.D.) and −8.31±21.02 ms (mean ± S.D.) in the initial contact and toe-off events, respectively. Additionally, with respect to the spatial features, the stride length and heel vertical displacement were overestimated by an average of 7.72 cm and 2.22 cm, respectively. We successfully extracted 17 gait features from two IMUs located on the foot. We have also demonstrated that symmetry index feature can distinguish normal healthy subjects and subject with recent history of lower-limb injury, which is important for clinical research.**

***Index Terms*—Gait analysis, inertial measurement unit, wearable sensor, multiple features.**

I. Introduction

GAIT analysis is the study of human locomotion and is usually performed in a laboratory environment. A comprehensive quantitative gait assessment is clinically useful as gait could be one of the markers for disease progression, it can characterize and distinguish asymptomatic gait, and track various rehabilitation progresses [1]–[5]. In sports applications, gait assessment is useful in tracking the performance of athletes, preventing injury, and providing training advice [6], [7]. Furthermore, in gerontology, gait assessment is used to predict the risk of falling in elderly people [8], [9].

Manuscript received March 16, 2020; revised May 4, 2020, July 12, 2020, and August 18, 2020; accepted August 21, 2020. Date of publication September 2, 2020; date of current version November 20, 2020. This article was recommended for publication by Associate Editor L. Zollo and Editor P. Dario upon evaluation of the reviewers' comments. This work was supported by Data Sciences Program II (DSP II) of Tohoku University and G-7 Scholarship Foundation. *(Corresponding author: Yonatan Hutabarat.)*

Yonatan Hutabarat is with the Neuro-Robotics Laboratory, Graduate School of Biomedical Engineering, Tohoku University, Sendai 980-8579, Japan (e-mail: y.hutabarat@neuro.mech.tohoku.ac.jp).

Dai Owaki and Mitsuhiro Hayashibe are with the Neuro-Robotics Laboratory, Department of Robotics, Graduate School of Engineering, Tohoku University, Sendai 980-8579, Japan (e-mail: owaki@tohoku.ac.jp; hayashibe@tohoku.ac.jp).

Digital Object Identifier 10.1109/TMRB.2020.3021132

Despite its usefulness, this systematic assessment is generally conducted in a laboratory environment using a specially designed gait analysis instruments, such as motion capture and force plate, and GaitRite [10]. However, the use of such specialized gait instruments is typically associated with drawbacks, such as the capture volume limitation using the motion capture system and the proportional relation between the number of gait cycles that can be captured and the number of instruments used (force plates/GAITRite); thus, a comprehensive gait assessment can only be performed in a specific motion laboratory with sufficient gait instruments. For this reason, wearable sensors have drawn interest from researcher in this field for their flexibility and relatively low-cost in comparison to lab-based gait instruments.

Several gait assessment studies have been conducted considering the use of wearable sensors. We identified several state of the art on this field as summarized in Table I. The first study [11] extracted step length, stride length, and gait speed using four inertial measurement unit (IMU) attached on both shanks and thighs based on inverted pendulum model, as well as three gait events, i.e., initial contact (IC), toe-off (TO), and mid-stance (MSt). Using the same number of sensors and placement, the second study [12] estimated step length while also identified three gait events, i.e., IC, MSt, and leg straightening (LS), as well as gait asymmetry feature based on double pendulum model. Model based algorithm has a set of assumptions and all parameters/inputs must be available to perform the algorithm. Comparison of using one IMU attached on waist and two IMUs on shanks were presented in [13]. It was concluded that using two IMUs on shanks leads to better accuracy in IC, stride time and step time features. The fourth paper [14] utilized only one IMU placed on foot and successfully detect heel-strike (HS), heel-off (HO) and TO events, and derived a number of spatial/temporal features (Table I). However, the experiment was done in treadmill which may disturb natural gait of participants [15], [16]. Other study [5] also investigated the use of one IMU placed on the lower back/fifth lumbar vertebrae (L5) and derived spatial/temporal features based on step activity instead of stride. Moreover, they also derived indices (asymmetry and variability) that can be used for clinical purpose such as in Parkinson's disease.

Research on gait assessment has widely been conducted. Nevertheless, many studies only focused on specific features rather than presenting a rich and diverse features that potentially could be extracted. In this study, we propose a framework to assess gait comprehensively with high-range of feature diversity using wearable sensors. Comprehensive here means

TABLE I
STATE OF THE ARTS OF GAIT ASSESSMENT USING WEARABLE SENSORS

Ref.	Sensor/Location	Gait event / Gait phase	Spatial/Temporal features	Other gait features	Validation
[11]	Four gyroscopes on shanks and thighs	IC, TO, MSt	Step length, Stride length, Gait speed	-	Instrumented mat
[12]	Four gyroscopes on shanks and thighs	IC, MSt, LS	Step length	Gait Asymmetry	Motion camera & tape measurement
[13]	One IMU on waist & Two IMUs on shanks	IC, FC	Step time, stance time, stride time	Coefficient of Variation	Pressure sensing insole
[14]	One IMU on foot	HS, HO, TO	Stride time, stance time, swing time, stride length, walking speed, incline	-	Footswitches and calibrated treadmill
[5]	One IMU on lower back	IC, FC	Step time, stance time, swing time, step length, step velocity	Asymmetry and Variability Indices	Instrumented walkway
Present Study	Two IMUs on feet	IC, TO, MSw, double support (DS)	Stride time, stance time, swing time, stride length, heel vertical displacement, gait speed, %gait phase, walking distance	Symmetry Index, Asymmetry Indices, Variability Indices, Activity class, Motion Intensity	Motion capture and force plates

extracting as many gait features as it possibly can, which includes gait event and/or phases detection, spatial and or temporal parameter extraction, and other related gait features. Table I represents the difference of feature diversity between our present study and the previous state-of-art works using portable sensors on gait assessment.

The rest of this article is organized as follows. Section II discussed about our proposed framework, experiments, and methods used in this study. Results and discussions are presented in Section III, which covers agreement between our proposed framework and lab-based measurement, overall quantitative gait assessment results, and comparison to several related study. Finally, Section IV concludes the study and provides direction of future research regarding this topic.

TABLE II
CHARACTERISTICS OF PARTICIPATED SUBJECTS

Subject	Age (years)	Height (cm)	Weight (kg)	Injury	Participation
S01	24	176	75	No	benchmark, walkway
S02	23	178	70	No	benchmark, walkway
S03	26	167	78	No	benchmark, walkway
S04	23	166	57	No	benchmark, walkway
S05	25	170	71	No	benchmark
S06	42	177	78	Yes	benchmark

II. METHODS

A. Subjects

Six subjects participated in the study with a mean age of 27.2±7.4 years and mean height of 172.3±5.3 cm and mean weight of 71.5±7.9 kg. Five of subjects reported that they have no severe lower limb related injuries in the past year, while one subject reported that he had injury on left foot and had performed a surgery regarding the injury five months prior to the experiment. Details of participated subjects are depicted in Table II. All subjects had given informed consent prior to participation to this experiments.

B. Data Collections

All subjects wore two IMU (Trigno Research+, Delsys, MA, USA) wireless systems on the back of the shoes as presented in Fig. 1. We selected this location as it was found to be the second best position in terms of accuracy for detecting the stride number [17]. We picked this location mainly for the purpose of practicality and convenience for the subjects, while also considering the accuracy results from the reference study. On the preliminary experiment of the reference study, the second best position outperformed all of other locations with 100% accuracy on detecting stride number based on accelerometer (compared to 96% accuracy from the best position). When tested to larger datasets (15 subjects) the accuracy was comparable to the best position, i.e., 93.60% for the best position vs. 93.20% for the 2nd best. In terms of convenience and practical issue, we think that placing it on the back of the shoes is the best option because we could reduce relative movement of the sensors without sacrificing the convenience of the subject that could alter their gait. If we were attaching it on the best position, we would need to make sure we attached the sensors securely with a Velcro belt that could be inconvenience to the subject and may alter their gait. In this study, the 3-axis accelerometer and 3-axis gyroscope data alone from each foot were considered. Motion capture system (Optitrack, NaturalPoint, OR, USA) and force plates (AMTI, MA, USA) were also used for benchmark experiment to assess the performance of the proposed system. The sampling rate of the IMU sensors was set at 148 Hz, whereas the motion capture system and force plate were sampled at 100 Hz and 1,000 Hz, respectively. IMU and force plate were down-sampled to 100 Hz for consistency of data analysis. All

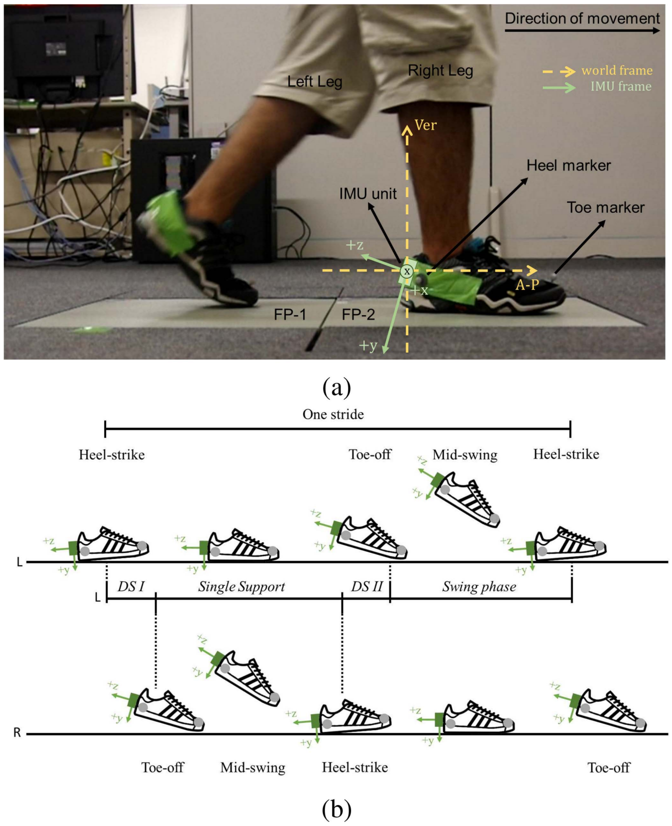

Fig. 1. (a) Experiment setup of our proposed framework, where IMU unit is attached on the back of the shoe. Two markers attached on heel and toe, and two force plates (FP-1 and FP-2) were used for benchmark experiment. IMU frame is transformed to world coordinates that consisted of vertical direction (Ver) and antero-posterior direction (A-P) for spatial features calculation. (b) Graphical presentation of IMU sensor placement (green box), marker placement (gray dot), and gait events and phases representation on both L(Left) and R(Right) foot.

the collected data were processed for analysis using MATLAB (Mathworks Inc., Natick, MA, USA).

C. Experiment Protocols

We developed two experiment protocols to assess the performance of our proposed methods. Experiments were divided into two stages, namely, benchmark and walkway experiments. The protocols and objectives for each experiment are described as follows.

1) Benchmark Experiment: Subjects were instructed to walk back and forth in a confined space defined by the area of motion capture system for 10 repetitions. Subject were instructed to adjust their walking speed to their own convenience and were encouraged to step their foot onto the force plate. These instructions were chosen owing to the fact that the capture area of the motion capture system was small thus the longest straight walking could only be 4.5 m. For this reason, to perform slow, normal, and fast walking would be ineffective. Heel markers were attached on the lateral side of each shoe, while toe markers were attached on the upper-front side of each shoe. The purpose of this experiment was to compare the performance of proposed framework in terms of gait event detection, as well as spatial/temporal parameters, with the ground truth, using a gold standard measurement from the motion capture and force plate system.

2) Walkway Experiment: Subjects were instructed to walk back and forth in a longer distance of 12 m for six repetitions at their own self-selected speed. The purpose of this experiment was to allow the subjects to walk more naturally, thereby providing an accurate assessment of each subject's natural gait.

TABLE III
OVERALL EXTRACTED FEATURES

Features (f)	Unit	Description
Stride time	s	Time needed to complete one gait cycle (IC to IC)
Stance time	s	Time elapsed when foot is in contact with the ground
Swing time	s	Time elapsed when foot is not in contact with ground
Stride length	m	Distance of one gait cycle
Heel vertical displacement	m	Estimated maximum height of heel during swing phase
Gait speed	m/s	Averaged walking speed of the subject
Walking distance	m	Total distance covered by subject
Gait phase	%	Percentage of average gait phase consisted of iDS, SS, tDS, SW
Symmetry Index	dimensionless	Symmetry feature based on stance time
Asymmetry Indices	multi	Various indices based on the absolute mean difference between sides (L&R)
Variability Indices	multi	Various indices based on standard deviation of certain features
Activity class	dimensionless	0 for other activities, 1 for walking, 2 for turning
Motion intensity	g	Intensity of motion based on magnitude of acceleration

D. Quantitative Gait Assessment

This section explains the overall procedure of the quantitative gait assessment (QGA) proposed in this study. As mentioned earlier, we used only two IMUs attached on the back of the shoes of each subject. Raw data from the IMU sensors were filtered using a 4th order Butterworth low pass filter with a cut-off frequency of 6 Hz. Following the filtering process, the data were processed according to the extracted gait features. The list of extracted features is presented in Table III.

1) Gait Event Detection: Gyroscope data were used to estimate three major gait events, i.e., initial contact (IC), toe-off (TO), and mid-swing (MSw). A heuristic-threshold based algorithm was constructed to detect these gait events. IC and TO were defined as the local maxima, whereas MSw was defined as the local minima detected from the gyro data. We set threshold of angular velocity, ω_n, 30 $\deg/s$ and $-120 \deg/s$ as the starting point to search for local maxima and local minima for IC, TO and MSw events detection, respectively. These values were based on the observational study during benchmark experiment. Flowchart of event detection is depicted in Fig. 2.

We computed angular acceleration, α_n, based on ω_n difference. When a local minimum is detected, marked by the change of sign in α_n, and ω_n is under the specified threshold

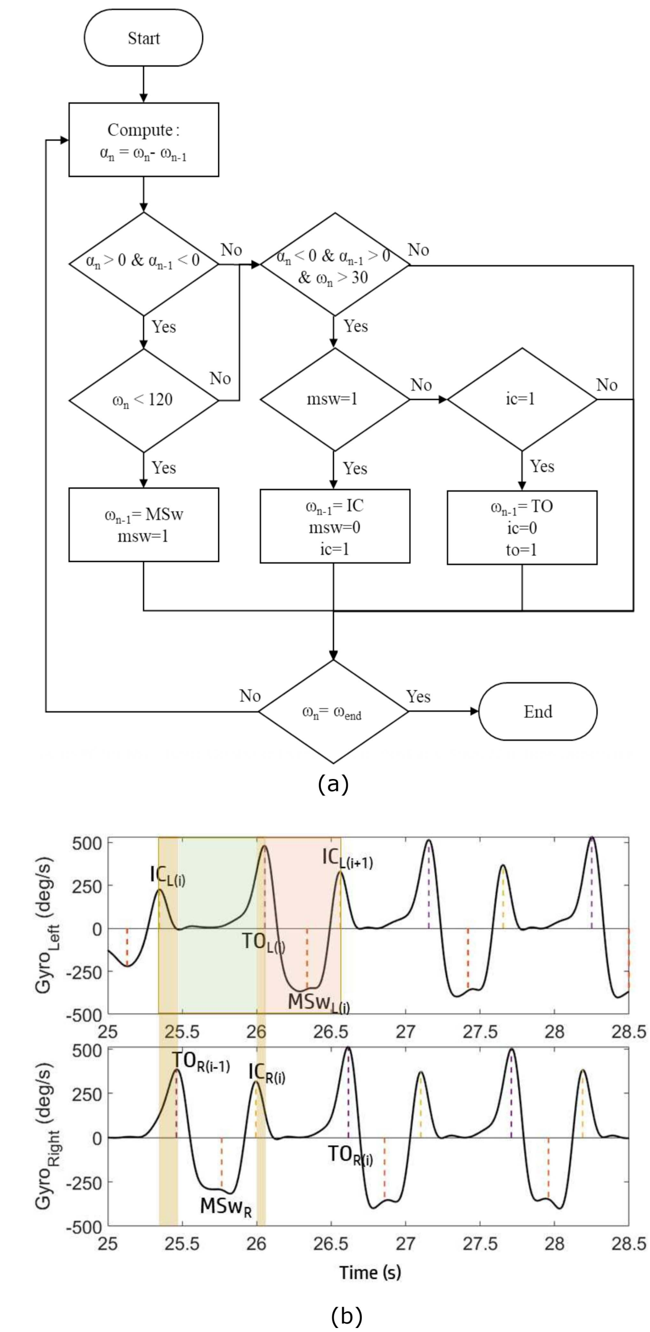

Fig. 2. (a) Flowchart of gait event detection based on gyroscope data on the back of the shoes. (b) Example of gyro data used for gait event detection. Dashed line indicates IC, TO, and MSw events. Shades indicate gait phases (yellow: double support, green: single support, red: swing).

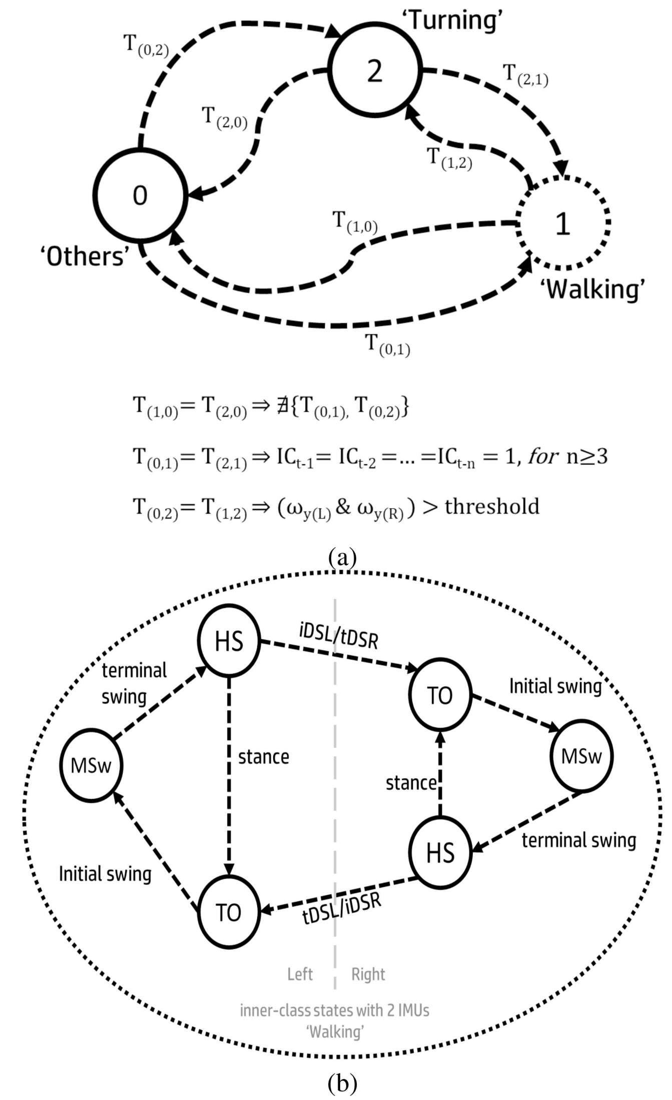

Fig. 3. (a) Activity class transition rules (b) Notation of inner-class states that could be recognized using the proposed framework.

of −120 deg /*s*, we marked the data sample as MSw and hold the value of 1 in *msw* variable. Meanwhile, when a local maximum is detected, also marked by the change of sign in α_n, and α_n is greater than the specified threshold of 30 deg /*s* and *msw* value is 1, then we marked the data sample as IC and reset the *msw* value as well as hold the value of 1 in *ic* variable. Otherwise, if there is another local maximum detected and *ic* value is 1, then we marked it as TO and reset the *ic* value and hold the value of 1 in *to* variable.

2) Activity Class: In this part of the study, we introduced three activity classes named walking, turning, and others class, to easily distinguish certain movements performed by the subjects. Certain thresholds were defined to construct a finite state machine (FSM) transition rule between the activity classes, as depicted in Fig. 3 (a). The movement performed will fall under 'walking' class if there are sequences of IC event detected. As two IMUs were used, the inner-class states could detect separately between left and right events, thus could lead to more detailed double support analysis in walking class. Terminology of inner-class states is represented in Fig. 3 (b), whereas the inner-class transition rules are presented in flowchart in Fig. 2. On the other hand, if there is a significant change, defined as a threshold of 250 deg /*s*, in longitudinal angular velocity in both of feet, movement will be categorized to 'turning' class. In this study, we classify turning as a class to record the changing of direction of the subjects and also to avoid inaccurate gait event detection and further spatio/temporal features calculation during transition to non-gait activity. Any movement performed that did not satisfy any of the above described states was classified as the 'others' class.

3) Temporal Features: Temporal features were derived based on gait event detection. Stride time was calculated by the time difference between detected ICs. Stance time was calculated by the time difference between detected TO and detected IC before the respected TO event, while swing time was calculated by the time difference between the detected IC after TO event and the respective TO event itself. Double support was estimated from the detection of IC of left side to the detection of TO of right side and vice versa. Initial and terminal double support, *iDS* and *tDS*, are interchangeable terms depending on the reference side. These descriptions are interpreted in Equation (1) to (5), where subscripts i, L and R are index of detected event, Left, and Right, respectively.

More over, we also present these temporal features in gait phase represented by percentage of each phase. Here we divided gait into four phases, consisted of iDS, SS, tDS, and SW, where SS and SW are single support and swing phase, respectively.

$$stride\ time = IC_{i+1} - IC_i \tag{1}$$

$$stance\ time = TO_i - IC_i \tag{2}$$

$$swing\ time = IC_{i+1} - TO_i \tag{3}$$

$$iDS_L = tDS_R = TO_R - IC_L \tag{4}$$

$$iDS_R = tDS_L = TO_L - IC_R. \tag{5}$$

4) Spatial Features: Spatial parameters were extracted from the combination of accelerometer and gyroscope data. We calculate stride length in quaternion system. Raw data from IMU sensor that are recorded in Euler angles, were transformed into quaternion. Accelerometer was rotated into Earth's frame and gravity component was compensated by subtracting transformed accelerometer data that is perpendicular with ground with g, where g is gravitational acceleration equal to 9.8 m/s^2. We followed a gradient descent algorithm [18] to estimate position based on IMU on quaternion system. This algorithm also include a magnetic distortion compensation algorithm and proven to reduce computational load. Further, we used a similar double integration method with [14], [19] to estimate velocity and lastly derived position. In this study, stride length is calculated per direction of walking to better estimate and avoid non-walking class data. On the other hand, we also introduced an estimation of heel vertical displacement (HVD) based on the transformed acceleration data to earth frame on vertical direction.

5) Other Gait Features: We also derived other gait features based on the extracted spatial and/or temporal features. Symmetry Index (SI) is a derived feature from stance time of both sides. We averaged total stance time of left side to right side for every walking class per experiment performed. Minus sign in SI indicates an overall less stance time on left side while positive sign indicates an overall less stance time on right side. Motion Intensity (MI) [20], [21] is a derived feature from the magnitude of the accelerometer data, which relates to the intensity of certain movement performed by the subject. Furthermore, it could be used to assess the difference of intensity between left and right side of the foot.

Additionally, we also extract Asymmetry Indices (AIs) and Variability indices (VIs) as studied in [5]. AIs are various indices based on the comparison of absolute mean difference between left (L) and right (R) side. These AIs could potentially give important information about subject specific tendency of using left and right foot in gait. VIs are features derived based on standard deviation. These features can provide an insight into the variability found on certain spatial/temporal features. SI, AI, VI, and MI are formulated in Equation (6) to (9), where n and f are number of gait cycle detected and spatial/temporal features, respectively. For example if f is stance time, then AI_f will be AI_{stance} where we calculate mean absolute error of stance time between left foot and right foot.

TABLE IV
PERCEPTION QUESTIONNAIRE

Subject	Benchmark Experiment		Walkway Experiment
	Perception	Step Adjusting	Perception
S01	Normal	Maybe	Normal
S02	Slower	Yes	Normal
S03	Normal	Yes	Normal
S04	Normal	No	Normal
S05	Slower	Yes	N/A*
S06	Normal	Maybe	N/A*

*N/A = Not Available (subject was not participated)

$$SI = \frac{\sum_1^n stancetime_L}{\sum_1^n stancetime_R} - 1 \tag{6}$$

$$AI_f = |mean(f_L) - mean(f_R)| \tag{7}$$

$$VI_f = S.D(f) \tag{8}$$

$$MI = |a| = \sqrt{a_x{}^2 + a_y{}^2 + a_z{}^2}. \tag{9}$$

III. Results and Discussion

We asked each of the participants about their perception of their gait during the experiment. Their responses have been summarized in Table IV. S02 and S05 stated that, during the benchmark experiment, they walked slower than normal, while other subjects stated that they perceived their gait as normal. As we only used two force plates, we encouraged all subjects to step on it every time they walked by. Only one participant, S04, declared that they did not need to adjust their steps on the force plate. Meanwhile on walkway experiment, all participated subjects stated that they walked normally. These subjective perception could be used as references to interpret the results that are discussed below.

A. Benchmark Experiment

A total of six subjects participated in this experiment. To synchronize motion capture, force plate system, and IMU sensors, all subjects performed jumping on the force plate (time was synchronized at maximum vertical acceleration from IMU and maximum vertical GRF from force plate). In addition to that, we introduced a bias correction of 0.07 s for time synchronization to IMU data based on the experiment trials. This correction factor is a lagging factor to compensate for the position of IMUs on feet that are not reflecting the acceleration of the whole body which correlates to the maximum GRF

TABLE V
SUMMARY OF BENCHMARK EXPERIMENT : QUANTITATIVE GAIT ASSESSMENT

Subject	Temporal features (s)			Spatial features (m)		Gaitspeed (m/s)	Gait Phase (%)				SI
	Stance time	Swing time	Stride time	Stride length	HVD		iDS	SS	tDS	SW	
S01	0.66±0.09	0.45±0.09	1.12±0.11	1.25±0.05	0.21±0.03	0.98±0.22	6.46	45.71	6.11	41.72	-0.032
S02	0.66±0.12	0.50±0.08	1.19±0.13	1.26±0.05	0.24±0.06	1.00±0.10	6.48	43.33	7.38	42.81	0.053
S03	0.65±0.21	0.45±0.15	1.18±0.24	1.12±0.04	0.21±0.05	0.89±0.15	8.59	42.27	8.76	40.39	0.068
S04	0.71±0.19	0.48±0.12	1.22±0.20	1.19±0.06	0.20±0.06	0.93±0.06	8.11	44.10	8.37	39.42	-0.018
S05	0.87±0.04	0.60±0.03	1.47±0.04	1.09±0.06	0.20±0.02	0.63±0.17	12.75	40.48	8.39	38.38	-0.039
S06	0.67±0.22	0.48±0.15	1.25±0.23	1.11±0.05	0.21±0.03	0.85±0.13	9.14	39.77	8.41	42.77	0.104

from the force plate. Further, we omitted the first continuous walking class until the first turning class and then started data analysis.

In terms of gait event detection reliability, the total of IC and TO events detected by force plates was 456 for all subjects. This number agrees with that obtained by our detection method based on IMU, exhibiting 100% detection rate. In total, we recorded 2286 gait events consisted of IC, TO, and MSw from all subjects during the benchmark experiment. We noticed there were a few missed or inaccurate event detection during the transition from walking to turning class and vice versa. This issue has been resolved automatically by introducing activity class, thus only IC, TO, and MSw during actual gait was recorded for analysis.

Table V summarizes a detailed gait assessment for each subject. Temporal features, spatial features, and gait speed are presented in mean ± S.D. Further more, we quantified gait phases in percentage of gait cycle, that could detail the iDS and tDS phases. Walking distance was not derived in this experiment as the walkway was short by approximately 4.5 m, and we did not explicitly instruct the subjects to follow a defined route or distance. Furthermore, for simplicity, we showed only SI among other proposed gait indices in this experiment as we focused on temporal/spatial agreement to the reference system and the comparison of our study to various existing studies. In term of stance time, S05 had the longest stance time and also the shortest stride length compared to other subjects, which resulted in the slowest speed among all subjects. Quantitative results from S05 showed an agreement with subject perception, as depicted in Table IV. We confirmed that the step adjusting effort by subject influenced the gait and resulted in slower speed than normal, as observed in S05. Table V indicates that the largest deviation of SI (SI = 0.104 or 10.4%) was found in S06. This finding was also correlated with the reported condition of S06 having lower limb injury.

Table VI summarized the agreement of benchmark experiment results of each participated subject to the reference system. Temporal and spatial differences between IMU and motion capture-based measurements are calculated in terms of mean and standard deviation. The negative sign indicates an early detection of temporal features and an overestimation of spatial features, while the positive sign indicates a late detection of temporal parameters and an underestimation of spatial features.

TABLE VI
BENCHMARK EXPERIMENT : AGREEMENT TO REFERENCE SYSTEM

Subject	Temporal Differences (ms)		Spatial Differences (cm)	
	IC	TO	Stride length	HVD
S01	9.74±8.54	-4.21±6.42	-9.59±4.56	0.27±3.50
S02	1.32±6.23	-15.53±8.91	-11.66±4.69	-4.32±6.00
S03	9.25±15.09	-15.50±43.2	-8.24±26.5	-3.54±6.24
S04	13.16±6.62	-7.63±10.76	-2.90±6.44	-5.08±5.50
S05	22.12±12.18	-0.30±7.70	-0.59±6.69	1.16±1.66
S06	12.89±7.68	-14.21±6.83	-10.93±5.73	-0.59±3.59
Average	4.22±15.48	-8.31±21.02	-7.72±12.8	-2.22±5.28

data is presented in mean±S.D

Table VI indicates that there was a 4.22±15.48 ms delay of IC detection and 8.31±21.02 ms early TO detection on average from all subjects. The lowest averaged temporal difference for IC and TO events was 1.32 ms and −0.31 ms observed from S02 and S05, respectively. On the other hand, we observed lowest temporal difference variability of 6.23 ms and 6.42 ms for IC and TO event from S02 and S01, respectively. Both lowest temporal differences and temporal differences variability are within one sampling time interval ($t_s = 0.01$ s). We observed that the variability of gait event timing for each subject is dependent on sensor placement and data filtering as has been reported in [17].

For spatial features comparison with motion capture system, we observed that our proposed method tends to overestimate by an average of 7.72±12.8 cm for stride length and 2.22±5.28 cm for estimated HVD, as summarized in Table VI). We observed the best overall agreement of spatial features in S05 where stride length and HVD are −0.59±6.69 and 1.16±1.66, respectively. Fig. 4. showed bland-altman plot on spatial features. It could be seen that mean level of all spatial features from all participated subject showing a minus sign, thus our proposed method on extracting spatial features showed a trend to overestimate spatial features.

Even using two IMU sensors, we confirm that temporal feature could be well identified compared to motion capture system with minor temporal differences. The spatial feature has some gaps due to the measurement accuracy difference compared to the global measurement system, however IMU-based stride length estimation can still capture the relative change of the gait, while having absolute spatial errors.

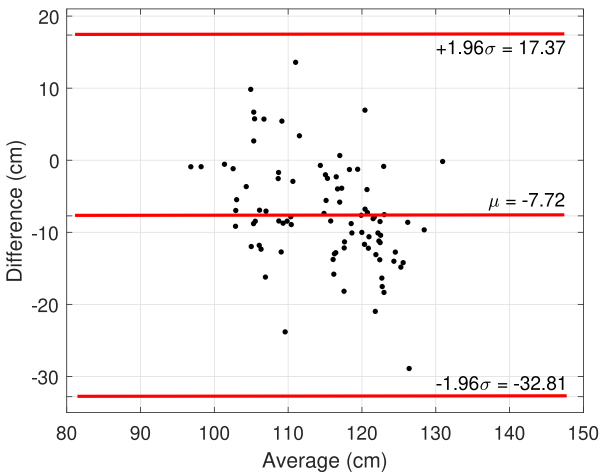

(a)

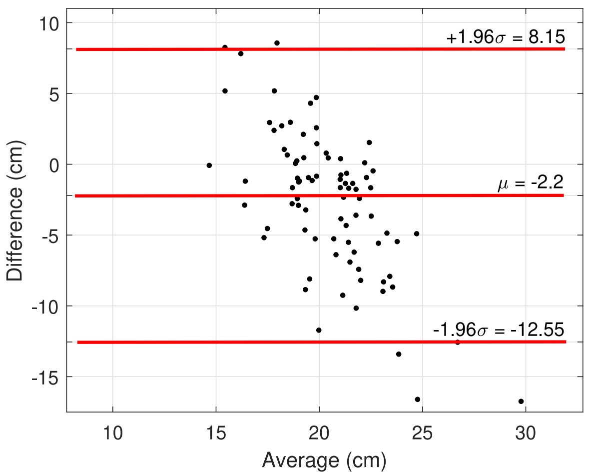

(b)

Fig. 4. Bland-Altman plot for spatial features. (a) stride length (b) heel vertical displacement. Red lines are mean, and range of limit of agreement (LoA).

However, in terms of HVD estimation, our proposed method suffered from inaccurate estimation that could reach 30% in terms of absolute error, even though we have implemented a linear correction algorithm based on all of the recorded gait data from all of the subjects. In our proposed method, for computational efficiency purposes, we estimated stride length and HVD in the same computation batch with IC as starting point. We found this became one of the factor contributing to the estimation error in HVD, as it should have been started from heel-off event instead of IC.

Furthermore, we compared our detection results with those of various existing studies in terms of temporal feature, as depicted in Table VII. Our results in IC detection performed better than all of previous studies, while TO detection performed better than [13], [14], and [22], [23]. To conclude, we have demonstrated that our proposed method provides an acceptable performance compared with those of various existing studies.

Table VIII compares our spatial features result with those of existing studies. Using four gyroscope and inverted pendulum model (IPM), as studied in [11] resulted in better estimation compared to reference system. In [17], the mean accuracy using the similar double-integration method as presented in this study was more than 90%, compared to our study which is 93.23 % of mean accuracy. A study on [26] also used the double-integration method with better accuracy and precision of 2 cm and 5 cm, respectively. The difference was sensor location (dorsum of foot) and the integration method that started from foot-flat event to next foot-flat event. Even though this location and method performed better in estimating stride length, it may not be suitable for determining gait events or stride number as shown on this study [17]. Study [25] used a deep-learning algorithm to estimate stride length, yet it took around 20 minutes per fold to train and a minimum of 4000 iterations to reach a stable error with precision, as shown in Table VIII.

TABLE VII
BENCHMARK EXPERIMENT : TEMPORAL DIFFERENCES COMPARISON TO EXISTING STUDIES PRESENTED IN MEAN±S.D.

Ref.	Sensor/ Location	Subjects	IC (ms)	TO (ms)
[13]	1 IMU (Gyro.)/ shank	10	12±11	51±21
	1 IMU(Gyro.+Acc.)/ L5	10	46±20	76±21
[14]	1 IMU(Gyro.)/ foot	5	70±N/A	35±N/A
[22]	2 Acc./ below knee	15	34±25	19±36
[23]	1 Gyro./ shank	7	-8±9	50±14
[24]	1 Gyro./ shank	9	-16.6±11.9	3.7±26.5
Present Study	1 IMU(Gyro)/foot	6	4.22±15.48	-8.31±21.02

N/A = Data not available ; Acc.=Accelerometer ; Gyro.=Gyroscope

TABLE VIII
BENCHMARK EXPERIMENT : STRIDE LENGTH COMPARISON TO EXISTING STUDIES PRESENTED IN MEAN±S.D.[CM] (%ACCURACY)

Ref.	Sensor/Location/Method	Subjects	Stride Length
[11]	4 Gyro./shanks&thighs/IPM	11	-2.7±N/A (N/A)
[17]	1 IMU/foot/Double-integration	15	N/A (≥90.00)
[25]	1 IMU/foot/Deep-learning	15	4.11±3.57 (N/A)
[26]	1 IMU/foot/Double-integration	10	2±5 (N/A)
	2 Gyro./shanks/SPM	15	-25.8±7.6 (N/A)
[27]	2 Gyro./shanks/DPM	15	3.8±6.6 (N/A)
	3 Gyro./shanks&thigh/DPM	15	-0.2±8.4 (N/A)
Present Study	1 IMU/foot/Double-integration	6	-7.72±12.8 (93.23)

N/A = Data not available ; Gyro.=Gyroscope

B. Walkway Experiment

A total of four subjects agreed to participate in the walkway experiment. This experiment focused on presenting subject-specific gait features that had been extracted using our proposed framework. Table IX shows an overall QGA based on our proposed framework.

We observed that all subjects took shorter time to complete a gait cycle, as seen from an overall less stride time in

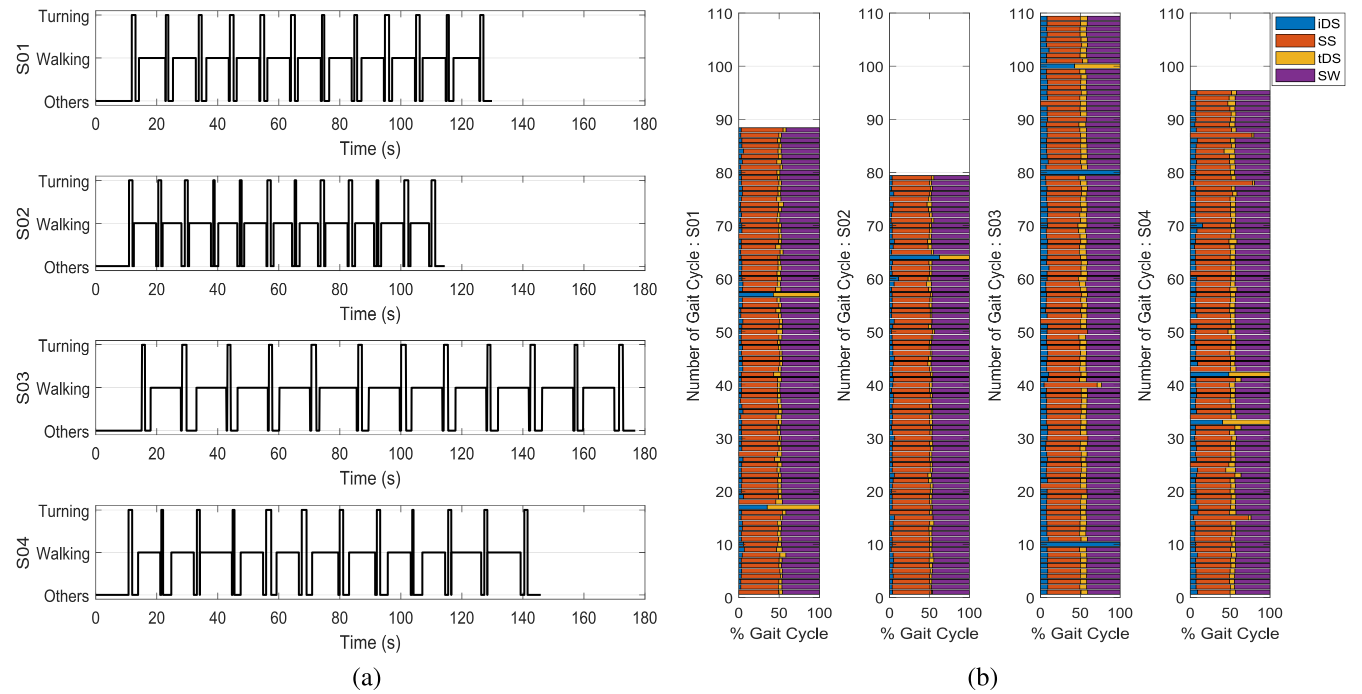

Fig. 5. Results from walkway experiment from all participated subjects, presented with same scale of time and number of gait cycle (a) activity class (b) number of gait cycles and detailed percentage of gait phases.

all subjects, compared to previous benchmark experiment. We also observed a longer stride length from all subjects compared to previous benchmark experiment. The walkway experiment was performed in a longer and wider space than the benchmark experiment, thus the walking distance was longer and the gait cycle time was shorter as subject tended to move in a more dynamic walking style. This slight change in walking style was well observed in our proposed method, which is a very important result as it demonstrates that the proposed method can accurately quantify the change of the gait under different environments. We can also note that both iDS and tDS time from all subjects were decreased in this experiment. This indicates that the subjects walks faster than during the benchmark experiment, which can be also observed in the gait speed feature.

We calculated the total walking distance covered by the subject based on stride length feature. We found that from 11 walking trials per subject in a 12 m walkway resulted in 11.92±1.07 m total distance covered per trial, with 95% confidence interval (CI) of [11.61, 12.24]. This confirmed that the accuracy of the proposed method for estimating stride length is the actual distance of 12 m with a 95% CI.

In terms of SI, we observed a good symmetry from all subject, $-0.03 < \mathrm{SI} < 0.005$, or not greater than 3% deviation from perfect symmetry ($\mathrm{SI} = 0$). In Table IX, we also verified AI and VI features based on all temporal features. Since two IMUs were used, we could detail the analysis for both left and right side of the foot based on these indices.

Fig. 5 shows activity class and detailed percentage of gait phases during walkway experiment. We presented the same scale of time and detected gait cycle to facilitate graphical comparison between subjects. Following the same protocols and overall walking distance, we observed that S02 was the fastest to complete this experiment, while S03 was the slowest. To further compare results between these subjects, we looked at number of stride (Fig. 5), stride length, stride time, double

TABLE IX
SUMMARY OF WALKWAY EXPERIMENT : SUBJECT-SPECIFIC QGA

QGA	S01	S02	S03	S04
Stance time (s)	0.56±0.09	0.54±0.07	0.65±0.26	0.61±0.19
Swing time (s)	0.48±0.08	0.47±0.06	0.45±0.11	0.45±0.08
Stride time (s)	1.05±0.09	1.02±0.07	1.13±0.25	1.08±0.19
Stride length (m)	1.50±0.08	1.54±0.16	1.30±0.07	1.46±0.12
HVD (m)	0.13±0.09	0.35±0.29	0.18±0.13	0.25±0.19
Gait speed (m/s)	1.42±0.08	1.49±0.17	1.15±0.08	1.36±0.15
Walking dist. (m)	134.03	115.44	142.5	132.67
iDS (%)	3.58	3.86	8.06	6.63
SS (%)	45.04	46.61	43.07	45.71
tDS (%)	4.35	2.91	7.45	6.23
SW (%)	47.03	46.62	41.43	41.42
SI	-0.029	-0.010	0.005	-0.018
AI_{stance} (s)	0.016	0.005	0.007	0.005
AI_{swing} (s)	0.014	0.000	0.005	0.001
AI_{stride} (s)	0.003	0.003	0.001	0.009
VI_{stance} (s)	0.016 (L) 0.021 (R)	0.011 (L) 0.016 (R)	0.017 (L) 0.016 (R)	0.020 (L) 0.027 (R)
VI_{swing} (s)	0.012 (L) 0.011 (R)	0.011 (L) 0.012 (R)	0.009 (L) 0.010 (R)	0.009 (L) 0.010 (R)
VI_{swing} (s)	0.029 (L) 0.029 (R)	0.021 (L) 0.027 (R)	0.021 (L) 0.020 (R)	0.023 (L) 0.034 (R)
MI_{swing} (g) *	2.02±0.14 2.03±0.18	2.19±0.13 2.12±0.16	1.83±0.13 1.72±0.13	2.08±0.31 1.98±0.26

*first row = Left ; second row = Right

support phase, gait speed, and also MI (Table IX) to clearly see the differences. In Fig. 5(b), we could observed that sometimes SS and SW is not detected and only show iDS and tDS. This occurrence happened not because of error in event detection, but merely shows a brief moment after turning, when both legs are on the ground, before the subject continue to walk. Furthermore, we could also correlate these result further with physical characteristics of the subject as presented in Table II, thus generating a detailed gait assessment.

In terms of speed coverage, range of speed are 0.63–1.00 m/s and 1.15–1.49 m/s for benchmark experiment and walkway experiment, respectively. Average transition speed from walking gait to running gait is around 2.00 m/s [28]. In that case we have covered and tested our proposed framework for roughly 0.63–1.49 m/s of walking speed and showed the accuracy and performance comparison to existing studies.

IV. Conclusion

We have investigated our proposed framework of quantitative gait assessment keeping a feature-rich diversity using only two IMU sensors. By decreasing numbers of sensors, we need to sacrifice the performance of gait assessment. Through the comparison to motion capture system and existing studies, we have verified the potential and the limitation of our proposed framework toward compact sensing system but with feature-rich diversity on gait assessment. We have successfully derived major gait events, IC, TO, and MSw, and gait phases that can provide detailed double support analysis in initial and terminal phases. The agreement of IC and TO events compared to lab-based motion capture and force plate system were 4.22 ± 15.48 ms delay on IC detection and -8.31 ± 21.02 ms early on TO detection, respectively. Meanwhile, for spatial features, our proposed approach tend to overestimate by an average of 7.72 ± 12.8 cm for stride length and 2.22 ± 5.28 cm for estimated HVD. We also discussed a detailed comparison to various existing studies and found trade-offs in performance between number of sensors used, sensor placement, and algorithms to extract spatial/temporal features. While our proposed framework (number of sensor+sensor placement+algorithms) could not achieve better performance in terms of all spatial/temporal features, we demonstrated that for some features, it performed better than some existing studies and generally could maintain a good accuracy. Moreover, we have successfully detailed iDS and tDS phases that could be employed for gait research. We also showed that preliminary validation presented in this study could clearly distinguished normal subjects and subject with a recent history of lower limb injury based on the SI, therefore indicates a potential use for clinical research. Detecting asymmetricity is an essential QGA for stroke patients or patients who use prosthetic leg. Another factor to be noted is the time spent for preparation, which can be significantly reduced using only two sensors. This provides an advantage for clinical purposes as we can not spend much time for patients in practical scenarios. Based on the results of the walkway experiment, we are confident that this framework can be implemented to monitor gait in a free-living environment, thus assessing the subject with their natural gait without space limitation. However, HVD estimation error could reach 30%. An advanced correction algorithm and/or different estimation method are needed to resolve this error. Even though we have successfully tested our proposed framework for roughly 0.63–1.49 m/s of walking speed, there are some slower and faster walking speed that we have not covered. For this reason, a better benchmark experiment that could incorporate slow, normal, and fast walking instruction could be done in the future to cover all possible walking speed. Another future works for this study would be testing our proposed approach for online application as well as testing it for wider audiences and combining the approach with other computational frameworks [29], [30] to expand the range of application toward general motion assessment.

Acknowledgment

The authors would like to thank Taku Sugiyama for helping with data collection on experiment trials for validation purposes.

References

[1] B. H. Dobkin, X. Xu, M. Batalin, S. Thomas, and W. Kaiser, "Reliability and validity of bilateral ankle accelerometer algorithms for activity recognition and walking speed after stroke," *Stroke*, vol. 42, no. 8, pp. 2246–2250, 2011.

[2] T. Ilias, B. Filip, C. Radu, N. Dag, S. Marina, and M. Mevludin, "Using measurements from wearable sensors for automatic scoring of Parkinson's disease motor states: Results from 7 patients," in *Proc. IEEE 39th Annu. Int. Conf. Eng. Med. Biol. Soc. (EMBC)*, Seogwipo, South Korea, 2017, pp. 131–134.

[3] C. Punin *et al.*, "A non-invasive medical device for Parkinson's patients with episodes of freezing of gait," *Sensors (Basel)*, vol. 19, no. 3, p. 737, 2019.

[4] C. Caramia *et al.*, "IMU-based classification of Parkinson's disease from gait: A sensitivity analysis on sensor location and feature selection," *IEEE J. Biomed. Heal. Inform.*, vol. 22, no. 6, pp. 1765–1774, Nov. 2018.

[5] S. Del Din, A. Godfrey, and L. Rochester, "Validation of an accelerometer to quantify a comprehensive battery of gait characteristics in healthy older adults and Parkinson's disease: Toward clinical and at home use," *IEEE J. Biomed. Health Inform.*, vol. 20, no. 3, pp. 838–847, May 2016.

[6] Y.-S. Lee, C.-S. Ho, Y. Shih, S.-Y. Chang, F. J. Róbert, and T.-Y. Shiang, "Assessment of walking, running, and jumping movement features by using the inertial measurement unit," *Gait Posture*, vol. 41, no. 4, pp. 877–881, 2015.

[7] Q. Mei, J. Fernandez, W. Fu, N. Feng, and Y. Gu, "A comparative biomechanical analysis of habitually unshod and shod runners based on a foot morphological difference," *Hum. Movement Sci.*, vol. 42, pp. 38–53, Aug. 2015.

[8] G. Rescio, A. Leone, and P. Siciliano, "Supervised machine learning scheme for electromyography-based pre-fall detection system," *Expert Syst. Appl.*, vol. 100, pp. 95–105, Jun. 2018.

[9] T. Virmani, H. Gupta, J. Shah, and L. Larson-Prior, "Objective measures of gait and balance in healthy non-falling adults as a function of age," *Gait Posture*, vol. 65, pp. 100–105, Sep. 2018.

[10] A. Caserta, P. Morgan, and C. Williams, "Identifying methods for quantifying lower limb changes in children with idiopathic toe walking: A systematic review," *Gait Posture*, vol. 67, pp. 181–186, Jan. 2019.

[11] E. Allseits, V. Agrawal, J. Lučarević, R. Gailey, I. Gaunaurd, and C. Bennett, "A practical step length algorithm using lower limb angular velocities," *J. Biomech.*, vol. 66, pp. 137–144, Jan. 2018.

[12] L. Wang, Y. Sun, Q. Li, and T. Liu, "Estimation of step length and gait asymmetry using wearable inertial sensors," *IEEE Sensors J.*, vol. 18, no. 9, pp. 3844–3851, May 2018.

[13] F. A. Storm, C. J. Buckley, and C. Mazzá, "Gait event detection in laboratory and real life settings: Accuracy of ankle and waist sensor based methods," *Gait Posture*, vol. 50, pp. 42–46, Oct. 2016.

[14] A. M. Sabatini, C. Martelloni, S. Scapellato, and F. Cavallo, "Assessment of walking features from foot inertial sensing," *IEEE Trans. Biomed. Eng.*, vol. 52, no. 3, pp. 486–494, Mar. 2005.

[15] L. H. Sloot, M. M. Van Der Krogt, and J. Harlaar, "Gait & posture self-paced versus fixed speed treadmill walking," *Gait Posture*, vol. 39, no. 1, pp. 478–484, 2014.

[16] M. D. Chang, S. Shaikh, and T. Chau, "Effect of treadmill walking on the stride interval dynamics of human gait," *Gait Posture*, vol. 30, no. 4, pp. 431–435, Nov. 2009.

[17] A. R. Anwary, H. Yu, and M. Vassallo, "Optimal foot location for placing wearable IMU sensors and automatic feature extraction for gait analysis," *IEEE Sensors J.*, vol. 18, no. 6, pp. 2555–2567, Mar. 2018.

[18] S. O. H. Madgwick, A. J. L. Harrison, and R. Vaidyanathan, "Estimation of IMU and MARG orientation using a gradient descent algorithm," in *Proc. IEEE Int. Conf. Rehabil. Robot.*, Zurich, Switzerland, 2011, pp. 1–7.

[19] Y. K. Thong, M. S. Woolfson, J. A. Crowe, B. R. Hayes-Gill, and D. A. Jones, "Numerical double integration of acceleration measurements in noise," *Meas. J. Int. Meas. Confed.*, vol. 36, no. 1, pp. 73–92, 2004.

[20] M. Zhang and A. A. Sawchuk, "A feature selection-based framework for human activity recognition using wearable multimodal sensors," in *Proc. BODYNETS 6th Int. ICST Conf. Body Area Netw.*, vol. 1, 2012, pp. 92–98.

[21] A. Derungs, C. Schuster-Amft, and O. Amft, "Physical activity comparison between body sides in hemiparetic patients using wearable motion sensors in free-living and therapy: A case series," *Front. Bioeng. Biotechnol.*, vol. 6, p. 136, Oct. 2018.

[22] R. W. Selles, M. A. G. Formanoy, J. B. J. Bussmann, P. J. Janssens, and H. J. Stam, "Automated estimation of initial and terminal contact timing using accelerometers; development and validation in transtibial amputees and controls," *IEEE Trans. Neural Syst. Rehabil. Eng.*, vol. 13, no. 1, pp. 81–88, Mar. 2005.

[23] B. R. Greene, D. McGrath, R. O'Neill, K. J. O'Donovan, A. Burns, and B. Caulfield, "An adaptive gyroscope-based algorithm for temporal gait analysis," *Med. Biol. Eng. Comput.*, vol. 48, no. 12, pp. 1251–1260, 2010.

[24] K. Aminian *et al.*, "Evaluation of an ambulatory system for gait analysis in hip osteoarthritis and after total hip replacement," *Gait Posture*, vol. 20, no. 1, pp. 102–107, Aug. 2004

[25] J. Hannink *et al.*, "Mobile stride length estimation with deep convolutional neural networks," *IEEE J. Biomed. Health Inform.*, vol. 22, no. 2, pp. 354–362, Mar. 2018.

[26] N. Kitagawa and N. Ogihara, "Estimation of foot trajectory during human walking by a wearable inertial measurement unit mounted to the foot," *Gait Posture*, vol. 45, pp. 110–114, Mar. 2016.

[27] A. Salarian, P. R. Burkhard, F. J. G. Vingerhoets, B. M. Jolles, and K. Aminian, "A novel approach to reducing number of sensing units for wearable gait analysis systems," *IEEE Trans. Biomed. Eng.*, vol. 60, no. 1, pp. 72–77, Jan. 2013.

[28] A. Rotstein, O. Inbar, T. Berginsky, and Y. Meckel, "Preferred transition speed between walking and running: Effects of training status," *Med. Sci. Sports Exerc.*, vol. 37, no. 11, pp. 1864–1870, 2005.

[29] R. De Souza Baptista, A. P. L. Bó, and M. Hayashibe, "Automatic human movement assessment with switching linear dynamic system: Motion segmentation and motor performance," *IEEE Trans. Neural Syst. Rehabil. Eng.*, vol. 25, no. 6, pp. 628–640, Jun. 2017.

[30] F. M. Ramos, A. d'Avella, and M. Hayashibe, "Identification of time-varying and time-scalable synergies from continuous electromyographic patterns," *IEEE Robot. Autom. Lett.*, vol. 4, no. 3, pp. 3053–3058, Jul. 2019.